Lifetime of the zero-voltage state in Josephson tunnel junctions

T. A. Fulton and L. N. Dunkleberger
Bell Laboratories, Murray Hill, New Jersey 07974
(Received 29 October 1973)

We describe an experimental investigation of fluctuations in the measured value of the critical current in Josephson tunnel junctions. The lifetime τ of the zero-voltage state against spontaneous transitions to a nonzero-voltage state is derived from these measurements. The range of τ covered by these measurements runs from 10^{-1} to 10^{-7} sec, with τ decreasing approximately exponentially with increasing current bias. Both thermal-noise-limited and extrinsic-noise-limited situations have been observed. In associated experiments the maximum critical current of these Sn–Sn-oxide–Sn juntions is found to be reduced from the value predicted by weak-coupling theory by a factor of ≈ 0.92, presumably by strong-coupling effects.

I. INTRODUCTION

The effect of noise on the properties of superconducting weak-link junctions has received considerable theoretical[1–9] and experimental[10–18] attention in recent years. Such studies are of intrinsic interest and also have technological importance in determining the limits of sensitivity of devices employing weak links. In this report we describe an experimental investigation of the effect of noise on the magnitude of the measured critical current I_{c0} in Josephson tunnel junctions, the archetype[19,20] of weak-link junctions. In the absence of noise, the current-voltage (I-V) characteristic of the junction would have a transition from $V=0$ to $V\neq 0$ at $I=I_{c0}=I_c$. Here I_c is the maximum Josephson supercurrent. (We assume throughout that no magnetic field effects occur.) Noise causes this transition to occur at various random values of I_{c0} smaller than I_c. For thermal noise this process can be described over a wide range of parameters in terms of a lifetime τ for the $V=0$ state, which is "metastable" against transitions to the $V>0$ state. The experiments give a direct determination of τ as a function of current bias in the range $10^{-1} \gtrsim \tau \gtrsim 10^{-7}$ sec. Both thermal-noise-limited and extrinsic-noise-limited values for τ have been observed depending on the screening of the electrical leads.

The electrodynamics of Josephson junctions are often treated in terms of an equivalent current-biased circuit comprising a capacitor C and resistor R in parallel with a supercurrent element, following the approaches of Stewart[21] and McCumber.[22] This model, which applies to junctions having negligible self-magnetic fields, has had success in explaining various features of junction behavior, such as the shape of the I-V curve. In this model the important parameter is $\omega_J\gamma$, where γ is the RC time constant and ω_J is the Josephson plasma frequency. Most theoretical treatments of noise in Josephson junctions have dealt with the overdamped regime $\omega_J\gamma \ll 1$, applying to point contacts, thin-film constrictions, and superconductor–normal-metal–superconductor sandwiches. For this regime predictions have been given by Ivanchenko and Zil'berman[1] and Ambegaokar and Halperin[2] concerning the effect of noise on the I-V curves. A number of workers[10–12] have investigated and confirmed these predictions experimentally in various junctions. Kurkijärvi and Ambegaokar[6] have carried out numerical calculations concerning the shape of the I-V curve for the underdamped regime $\omega_J\gamma \gg 1$, which applies to Josephson tunnel junctions in most common experimental situations. Previous experiments[10,23] on noise effects in tunnel junctions have used the overdamped picture. Noise-induced modification of the I-V curves of tunnel junctions at $V\neq 0$ may be expected to be relatively minor for $\omega_J\gamma \gg 1$, compared to the effects on overdamped junctions. The most visible effect of noise involves the reduction of the measured critical current from its theoretical maximum. For this process the theory involves merely thermal excitation over an energy barrier,[4,24–26] and consists of a simple activation picture with a single attempt frequency and an exponential dependence on the activation energy and temperature. It is this process which is investigated here. While many workers have mentioned this effect and it has often been suggested as an explanation for observed critical currents smaller than theoretically expected,[27] we are not aware of any previous systematic studies.

Investigations of the noise-induced decay of the metastable zero-voltage states in point-contact weak-link junctions have previously been carried out by Jackel, Kurkijärvi, Lukens, and Webb.[13,14] These workers investigated the transitions between neighboring circulating-current states of a point contact in a superconducting ring and obtained good agreement with theory.[7] The physical mechanism for their phase-slippage events is noise-induced activation over an energy barrier. The present

studies investigate the same mechanism in an underdamped regime, and thereby complement the studies of the overdamped point-contact junctions. For tunnel junctions one can determine independently the capacitance and critical current of the junction. This allows a slightly more direct comparison of theory and experiment than is possible for point contacts. The present work also employs an analysis of the data in terms of lifetimes rather than line shapes, which somewhat simplifies comparison with theory. Finally, the experiments with tunnel junctions are much easier to perform than the point-contact work because the signal levels are much larger.

II. THEORY

The Stewart-McCumber[21,22] equivalent-circuit model of a current-biased tunnel junction is shown in Fig. 1(a). The bias current I is shared by the resistance R, capacitance C, and the supercurrent element through which a current $I_c \sin\varphi$ flows. Here I_c is the Josephson critical current and φ is the well-known phase difference operative in the Josephson effect. The current-continuity equation is

$$I = I_c \sin\varphi + \frac{V}{R} + C\frac{dV}{dt} \ , \tag{1}$$

where V is the voltage across each element. Using Josephson's second equation, $2\pi V = \Phi_0 d\varphi/dt$, where $\Phi_0 = 2.068\times10^{-15}$ Wb is the flux quantum, (1) becomes

$$x = \sin\varphi + \frac{1}{\omega_J^2\gamma}\frac{d\varphi}{dt} + \frac{1}{\omega_J^2}\frac{d^2\varphi}{dt^2} \ . \tag{2}$$

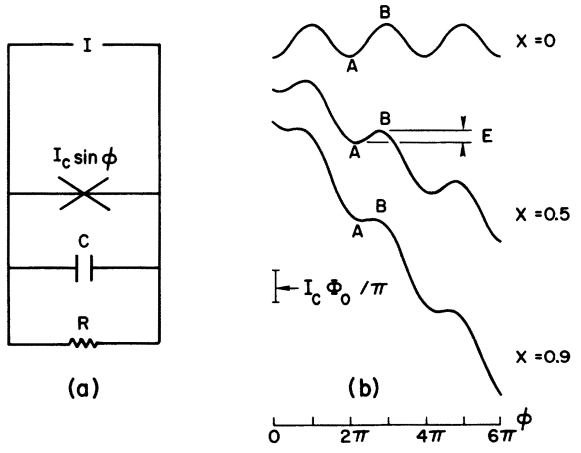

FIG. 1. (a) Stewart-McCumber circuit model for Josephson junctions. (b) Potential energy vs φ for current-biased junctions where $x = I/I_c$. The potential-energy difference between points A and B is E, the energy barrier.

This familiar second-order nonlinear differential equation determines the time dependence of φ and hence the voltage and currents. Here $x = I/I_c$, $\gamma = RC$, and $\omega_J = (2\pi I_c/\Phi_0 C)^{1/2}$.

As is well known, the behavior predicted by this equation is easily visualized in terms of a mechanical analog, e.g., that of a particle moving in a potential energy of the form $(-x\varphi - \cos\varphi)$, where φ is the particle position. In what follows we will sometimes employ mechanical terms to illustrate a particular behavior of the junction. Figure 1(b) shows potential-energy curves of this form. The energy is expressed in units of $I_c\Phi_0/\pi$, the Josephson coupling energy, which is the maximum potential-energy variation that can occur in the junction at $x = 0$.

In the underdamped limit, $\omega_J\gamma > 1$, and if $(\omega_J\gamma)^{-1} \ll x < 1$, the steady-state behavior of the junction is simple. Either the junction is constrained to remain in a particular potential minimum [e.g., point A in Fig. 1(b)], at and around the value of $\varphi = \sin^{-1}x$, or, alternately, the junction is "free running" with its phase increasing at a rate of $d\varphi/dt = 2\pi IR/\Phi_0$; i.e., $V = IR$. In the mechanical analog the particle is either at rest in a potential minimum or rolling steadily downhill at a rate determined by the average slope and the damping, with a kinetic energy greatly exceeding the modulation depth of the potential. This regime is generally taken as describing the tunnel junction, with the added consideration that the parallel resistance is nonlinear in voltage, corresponding to the well-known quasiparticle I-V curve.[28]

The addition of thermal noise to this problem is often simulated[1,2,6] by adding to the dc current I, a noise current characteristic of the parallel resistance R at a temperature T. It seems probable that such noise currents would have little effect in the steady-state $V > 0$ condition of an underdamped junction, except for $x \sim (\omega_J\gamma)^{-1}$. If the junction is initially in the $V = 0$ steady state, the noise currents cause the junction phase to oscillate within the boundary of the potential well, and ultimately to escape from the well, usually over the energy barrier on the lower side [point B in Fig. 1(b)]. The junction then either will be retrapped in a subsequent potential well or will switch into the free-running $V \neq 0$ state. If the effect of noise-induced retrapping is ignored, the junction will go to the $V \neq 0$ state if $x \gtrsim (\omega_J\gamma)^{-1} \ll 1$, since the damping is too small to remove the "kinetic" energy that the junction acquires from the applied current in the escape over the first barrier. The probability of noise-induced retrapping[6] is difficult to assess. We shall examine this question later, but for the moment we assume that it is negligible and that the result of a single noise-induced escape from a potential well is an experimentally large effect;

namely, the junction voltage jumps from $V=0$ to the gap voltage 2Δ (~1 mV for Sn).

Provided the activation rate from the potential well is small compared to ω_J, so that the energy distribution of the junction prior to the activation is near-thermal, the activation rate at fixed x can be characterized[4,7,24–26] by a constant probability/unit time

$$\tau^{-1} = (\bar{\omega}_J/2\pi)\, e^{-E/kT} , \tag{3}$$

where τ is a lifetime for the metastable $V=0$ state. Here E is the energy barrier of Fig. 1(b) and depends upon I and I_c according to

$$E = (I_c \Phi_0/2\pi)[x(2\sin^{-1}x - \pi) + 2\cos(\sin^{-1}x)] , \tag{4}$$

which is shown in Fig. 2. This function decreases linearly with x at small x according to $d(\ln E)/dx = -\frac{1}{2}\pi$, and for values of x approaching unity is well approximated by $E = (\Phi_0 I_c/3\pi)(2-2x)^{3/2}$. The angular attempt frequency[24] $\bar{\omega}_J$ depends on I and I_c according to

$$\bar{\omega}_J = \omega_J(1-x^2)^{1/4} , \tag{5}$$

where we have assumed $\omega_J \gamma \gg 1$. While expression (3) only applies strictly to thermal noise, in situations in which extrinsic noise is important it is probably still meaningful in most cases to attribute a probability/unit time τ^{-1} for noise-induced escape from the potential well. In this case expression (3) might still apply with an effective noise temperature T_N larger than the true temperature, but probably only if the external noise had a constant spectral density.

Experimentally one starts with the junction in the $V=0$ state at $I=0$ and increases I steadily. At some point the junction switches from $V=0$ to $V \neq 0$. This value, the observed critical current denoted I_{c0}, is of course less than I_c due to the noise. Further, since the noise-induced activation occurs as a random event with an average rate dependent on I, the value of I_{c0} takes on random values with a certain probability distribution. This distribution, denoted by $P(I)$, is defined by the condition that the probability that I_{c0} will occur in a small current interval ΔI between I and $I+\Delta I$ is $P(I)\Delta I$. The experiments thus produce directly $P(I)$, which contains information on the more fundamental $\tau^{-1}(I)$.

Obviously $P(I)$ depends both on $\tau^{-1}(I)$ and on the form and frequency of the current sweep. Kurkijärvi[7] has given predictions for a very similar probability distribution in the case of metastable circulating-current states of a ring of inductance L closed by a Josephson junction and subject to a time-varying external flux. The measurements of of Refs. 13 and 14 were analyzed by comparison with these predictions. Specifically, Kurkijärvi has considered the probability of a jump occurring

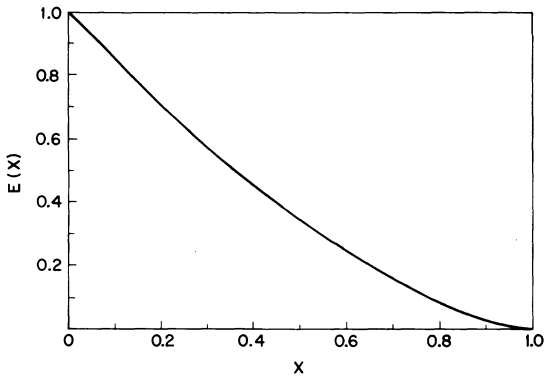

FIG. 2. Theoretical dependence of E on x. E is measured in units of $I_c\Phi_0/\pi$.

at a particular applied flux from one such state to a lower-energy neighboring state as a result of thermal noise. In the limit $LI_c/\Phi_0 \gg 1$ this probability is essentially the same as $P(I)$ in the present case, and his predictions, which correspond to $x \lesssim 1$ and linear current sweep, could be used to compare $P(I)$ with theory.

An alternate and perhaps more convenient approach is to transform $P(I)$ directly into $\tau^{-1}(I)$. The relation between the two is

$$P(I) = \tau^{-1}(I)\left(\frac{dI}{dt}\right)^{-1}\left(1 - \int_0^I P(u)\,du\right) , \tag{6}$$

where $P(I)$ is normalized to unity. We find it useful to understand this expression in terms of an ensemble of junctions subject to increasing I. In this picture the final factor in (6) represents the number of junctions remaining in the $V=0$ state after the current bias has reached the value I. Since $P(I)$ is experimentally known and $I(t)$ is known (sinusoidal in our case), $\tau^{-1}(I)$ can be obtained directly.

III. EXPERIMENTS AND DATA REDUCTION

A. Junction preparation and preliminary experiments

The tunnel junctions were cross-type Sn–Sn-oxide–Sn thin-film sandwiches prepared on glass substrates by standard evaporation procedures. Areas ranged from ~4×10^{-5} to $<10^{-6}$ cm^2 and film thicknesses were ~3000 Å. Oxides were formed *in situ* by dc oxygen-plasma dischange.

Each sample was initially mounted on a sample holder and electrical leads were attached for four-terminal measurements of the I-V curve. These were recorded at ~1.5 K by photographs of an x-y oscilloscope display and/or x-y recorder plots. At this stage any junction exhibiting anomalously large ($\gtrsim 1\%$) current flow at voltages below the energy gap 2Δ or other anomalies was discarded. Figure 3 shows an I-V curve of what was regarded

as an acceptable junction.

For acceptable junctions a pair of digital voltmeters was used to record the value of the current drawn by the junction at a voltage bias of 3 mV. As described subsequently, this quantity was used to calculate a predicted value for I_c.

B. Measurement of $P(I)$

Measurements of the $P(I)$ distribution were carried out on about ten different junctions with predicted values of I_c in the 1–20-μA range, corresponding to normal-state resistance of ~50–1000 Ω. For these measurements the junctions were usually switched from the first sample holder to one in which the electrical leads were provided with additional electrical shielding. In the simplest and most successful design the samples were mounted inside a brass exchange-gas chamber immersed in liquid He and supported from the top of the Dewar by a stainless-steel tube. A single copper electrical lead within the tube was used to make two-terminal I-V measurements on the sample, using the supporting tube as the electrical return. This electrical connection to room temperature approximated a simple coaxial transmission line. In principle, radiation from room temperature or other extrinsic-noise sources could be attenuated[29] by making the center cable conductor of a high resistance per unit length. To roughly approximate this condition two wire-wound 1000-Ω resistors were incorporated into the center lead inside the tubing at the low-temperature end, near the sample. Additionally, the hole through which the coaxial line emerged into the sample chamber was tightly wrapped with Al foil to provide an impedance discontinuity. Although the attenuation of noise broadcast down the coaxial line by this simpleminded arrangement would be difficult to predict *a priori*, experimentally it seems to have been sufficient to reduce the effect of extrinsic noise to a relatively small fraction of the effect of the intrinsic thermal noise.

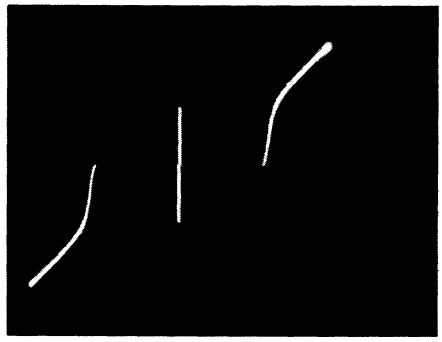

(a)

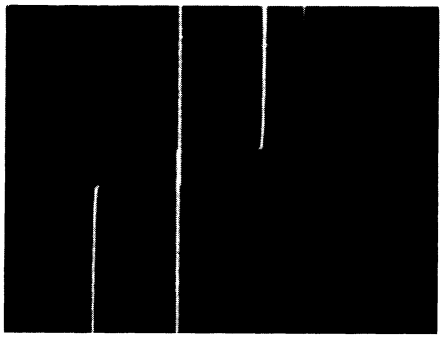

(b)

FIG. 3. Current-voltage characteristics of junction 31A-5-9. (a) 500 μA/vertical division and 0.5 mV/horizontal division. (b) 10 μA/vertical division and 0.5 mV/horizontal division. Temperature = 1.4 K.

At the room-temperature end, the precautions taken against external noise involved the use of coaxial current and voltage leads throughout, the use of battery-powered amplifiers and oscillator where possible, and the enclosing of the experiment in a shielded room.

The two leads to the sample were wired at the room-temperature end for four-terminal I-V measurements. The current bias, provided by a battery-powered audio-frequency oscillator with 0.1-MΩ impedance, was sinusoidal in time with amplitude $I_m \sim (1.2\text{–}2) I_{c0}$. The I-V curve of the series combination of the tunnel junction and the 2000-Ω screening resistors was displayed on an oscilloscope. Since the junctions were of fairly high resistance, the ~1-mV voltage jumps at I_{c0} were clearly visible despite the sloping background.

The current supplied to the junction passed through a 5000- or 10000-Ω sampling resistor and the voltage from this resistor was amplified by a Princeton Applied Research 113 amplifier and supplies to a Nicolet 1074 multichannel signal averager with a type SW-75 voltage-distribution analyzer (VDA) plug-in. The junction voltage was amplified by a second PAR 113 amplifier and supplied to the trigger of a pulse generator. The 0.1-μsec pulses from this generator were used in turn to trigger the "sample" command of the VDA.

The trigger level of the pulse generator was so adjusted as to trigger whenever the junction jumped from $V = 0$ to $V \neq 0$. The VDA would then sample the value of the voltage from the current-measuring resistor and add a single count to that channel whose address corresponded to the sampled voltage. In this way a distribution of counts versus channel number was collected which formed the histogram equivalent of $P(I)$.

Calibration of the channel number in terms of current were determined to $\approx 1\%$ by supplying a known dc current through the sampling resistor in the actual measuring setup. A typical resolution

used was ≈ 8.85 nA/channel, giving a range of ~10 μA in the 1024 channels of the signal averager. Location of the channel numbers corresponding to $I=0$ and $I=\pm I_m$ could be conveniently obtained by letting the pulse generator run at a fixed rate. The random samples produced a $(\cos)^{-1}$-like histogram whose extreme values correspond to $I=\pm I_m$.

Sweep frequencies were usually set in the range of ~300 Hz and counting times ~80 sec, giving typically ~2000 counts/channel at the peak of the distribution. In principle counting rates up to 10 kHz could be, and sometimes were, used to give improved statistics and to extend measurements to shorter lifetimes, but the phase shifts encountered at the higher frequencies tended to shift and distort the distribution by a few channels, and sufficiently good statistics could be obtained at the lower frequencies.

A typical experimental run involved recording of such histograms for a particular junction at perhaps ten different temperatures in the range 3–1.3 K. On occasion the effect of magnetic field was also examined, but since the relation between I_c and field depends on the unknown details of the geometry of the junction, no quantitative comparisons with theory were attempted for data taken at nonzero fields.

C. Preliminary data reduction

The data as recorded by the VDA are a histogram showing the number of counts $P(K)$ in the channel K. To obtain $\tau^{-1}(I)$ we first associate a current $I(K)$ to channel K by using the calibrated current interval per channel (denoted ΔI) and the measured channel number corresponding to $I=0$. We can also determine the current sweep rate dI/dt corresponding to channel K since we know the sweep frequency and the channel numbers corresponding to I_m. We denote by $K=1$ the channel corresponding to the highest value of I_{c0} in the distribution. Then $\tau^{-1}(K)$ is computed according to the formula

$$\tau^{-1}(K)=\frac{dI}{dt}\,\frac{1}{\Delta I}\,\ln\left(\sum_{j=1}^{K}P(j)\Big/\sum_{i=1}^{K-1}P(i)\right). \qquad (7)$$

This is equivalent to approximating $\int_I^\infty P(u)\,du$ by a series of exponentials fit between adjacent points of $\sum_{j=1}^{K}P(j)$, effectively assuming thereby that $\tau^{-1}(I)$ is constant over a single-channel interval. An exponential fit is used rather than a linear fit because the values of $P(K)$ may decrease quite abruptly for low values of K. Finally, $\tau^{-1}(K)$ is assigned to $I(K)$ to yield $\tau^{-1}(I)$.

A set of three histograms $P(K)$ obtained at different temperatures for the highest-resistance junction studied are shown in Fig. 4 (junction N22B-6-8). Immediately above each histogram is a curve of $\log_{10}\tau^{-1}(I)$ obtained as described. The observed

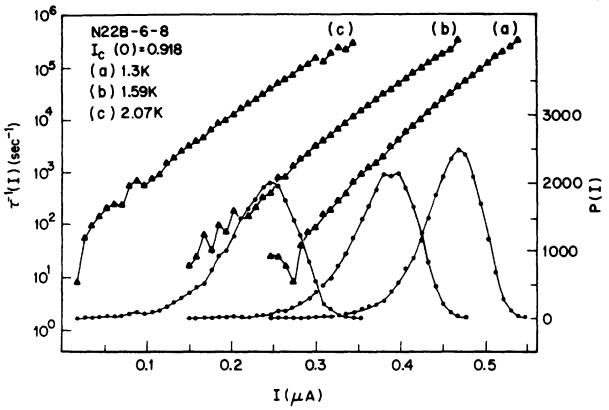

FIG. 4. $P(I)$ and $\log_{10}\tau^{-1}(I)$ vs I for junction N22B-6-8. Sweep frequency was 289 Hz and sweep amplitude was 0.92 μA.

lifetimes cover the range from ~10^{-1} to ~10^{-6} sec, decreasing steadily and approximately exponentially as I increases. As we shall see in Sec. III D, these curves are in fairly good agreement with predictions of the thermal activation theory. By using higher sweep frequencies such measurements on this and other junctions have extended the observed lifetimes to $\approx 10^{-7}$ sec. No unusual behavior was observed at these lifetimes, which are comparable to RC for these junctions.

D. Critical-current determination

To analyze the measured $P(I)$ the true value of the critical current I_c had to be determined as well as the capacitance C. These quantities were needed to determine the energy barrier and the plasma frequency. We describe here our procedure for this.

Neither quantity could easily be measured on the high-resistance junctions in which $P(I)$ was most usefully studied, since I_{c0} was substantially reduced from I_c in such junctions and the Fiske steps[30] which could be used to measure C were usually not observable at all. Consequently, we adopted the approach of determining I_c and C in a series of low-resistance junctions and extrapolating from these values to determine I_c and C for the high-resistance junctions.

According to numerical calculations[31] based on the theory of Ambegaokar and Baratoff,[32] the value of I_c for a Sn-Sn junction at $T=0$ should be $I_c=f(\pi\Delta/2R_N)$, where Δ is the energy gap of Sn, R_N is the normal-state junction resistance, and $f=0.911$ is the strong-coupling factor. As this value of f for Sn has recently been subject to experimental question,[33] we adopted the following heuristic procedure for determining I_c. A series of junctions in the range 1–10 Ω was investigated at temperatures

from 1.4 to 1.5 K and the current drawn by the junction at a voltage bias of 3.00 mV [denoted I (3 mV)] was measured using a pair of digital voltmeters. The measured critical current I_{c0} for junctions in this resistance range was expected and observed to be defined to $<1\%$. To measure I_{c0} a combined audio-frequency current of amplitude I_{ac} and a dc current I_{dc} were applied to the junction. The value of I_{dc} was swept slowly from $I_{dc} > I_{c0} + I_{ac}$ to $I_{dc} < -I_{c0} - I_{ac}$, and the average junction voltage $\langle V \rangle$ was recorded versus I_{dc} on an x-y recorder. The hysterisis of the I-V curve produced four well-defined jumps in $\langle V \rangle$ versus I_{dc} in this range, at the values $I_{dc} \pm I_{ac} = \pm I_{c0}$ and $I_{dc} \mp I_{ac} = \pm I_0$, where $\pm I_0$ are the currents at which the I-V curve returns from $V \neq 0$ to $V = 0$. The value of I_{c0} could be obtained by subtracting I_0 ($\lesssim 1\%$ of I_c). An extrapolated value of I_{c0} at $T = 0$ was obtained by assuming[32] $I_c(T)/I_c(0) = [\Delta(T)/\Delta(0)] \tanh[\Delta(T)/2kT]$ and using tables of Mühlschlegel.[34] The ratio of $I_{c0}(T=0)/I$(3 mV) was then evaluated for that junction.

Figure 5 shows the results of this measurement for 11 randomly selected good-quality junctions. The points are the $I_{c0}(T=0)/I$(3 mV) with error bars which represent our uncertainties in measurement, most of which occur in measuring I_{c0}. Even for these relatively low-resistance junctions, I_{c0} is necessarily somewhat smaller than I_c due to noise. Roughly this depression is 1–2%, depending on I_c and on the unknown noise level of the particular sample holder (estimated at ~4 K). Somewhat arbitrarily, then, we have chosen to use the value I_c/I(3 mV) = 0.301 for predictions of I_c for the high-resistance junctions, a value which we feel is accurate to about 1%.

These measurements can be used as a determination of the strong-coupling factor f mentioned previously, although since the gap values 2Δ vary from sample to sample, the accuracy is less than that of I_c/I(3 mV). Let us denote by $\bar{R}$ the resistance (3 mV)/I(3 mV). By warming the junctions to just below T_c ($2\Delta \sim 0.1$ mV) and taking the slope of the I-V curve in the 2–5-mV range at this temperature to be equal to R_N, we have measured $\bar{R}/R_N = 1.0335 \pm 0.0010$ on four different junctions. If we choose 2Δ for Sn to be 1.21 mV, the value for f corresponding to $I_c(T=0)/I$(3 mV) = 0.301 is $f = 0.919$. Such a value is in approximate agreement with the numerical calculations of the theory, but disagrees with the measurements of Ref. 33.

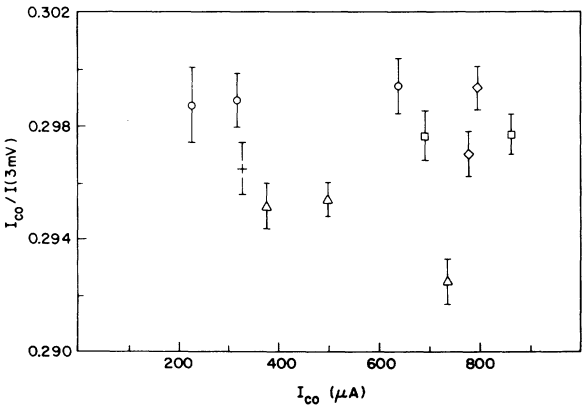

FIG. 5. I_{c0}/I(3 mV) for 11 different junctions, including that of Fig. 3. Points with the same symbol are for different junctions fabricated simultaneously on the same substrate.

To determine the value of C we measured the voltage of the fundamental Fiske steps induced by application of a magnetic field in eight low-resistance junctions. From these and a knowledge of the junction dimensions we obtained $\bar{c}$, the velocity of electromagnetic propagation in the junction structure. The average value measured for $\bar{c}$ was $(1.2 \pm 0.1) \times 10^7$ m/sec at frequencies in the range of 300 GHz. Assuming a value of 1300 Å for the magnetic thickness of the junction (twice the penetration depth plus the oxide thickness), we obtain a value of 2.08 ± 0.2 Å for the effective-junction oxide thickness divided by the dielectric constant.[35]

This value is of course not fixed, but varies with junction resistance in a logarithmic way. We neglect this unknown but weak dependence for simplicity, as variations in the plasma frequency provide only a relatively weak dependence in the predicted behavior.

IV. ANALYSIS

A. Near-intrinsic noise

Figure 6 shows data taken at four temperatures for junction N22B-4-10, plotted as $\log_{10} T^{-1}(I)$ versus $E(I)$. The energy barrier $E(I)$ was calculated from (4) using $I_c(T=0) = 0.918\ \mu\text{A} = 0.301 I$(3 mV) with corrections to finite temperature made using[32] $I_c(T)/I_c(0) = [\Delta(T)/\Delta(0)] \tanh[\Delta(T)/2kT]$. Curves (a)–(c) correspond to the $P(I)$ of Fig. 5. The error bars for the energy correspond to 1.5 channel numbers, and arise from a random one-channel displacement observed in repeated recordings of the same $P(K)$ combined with a one-channel number uncertainty in the position of $I = 0$. Systematic errors of the order of 1% could also result from the calculation of I_c, the calibration of the current interval per channel, and a slight phase shift in the current-sampling voltage at the 300 Hz sweep frequency. Statistical errors in the $P(K)$ are ~2% at the peaks.

To obtain a feeling for the energies involved and the validity of comparisons with theory for these data, we may go over briefly some of the numbers for curve (c), Fig. 6. At this temperature of T

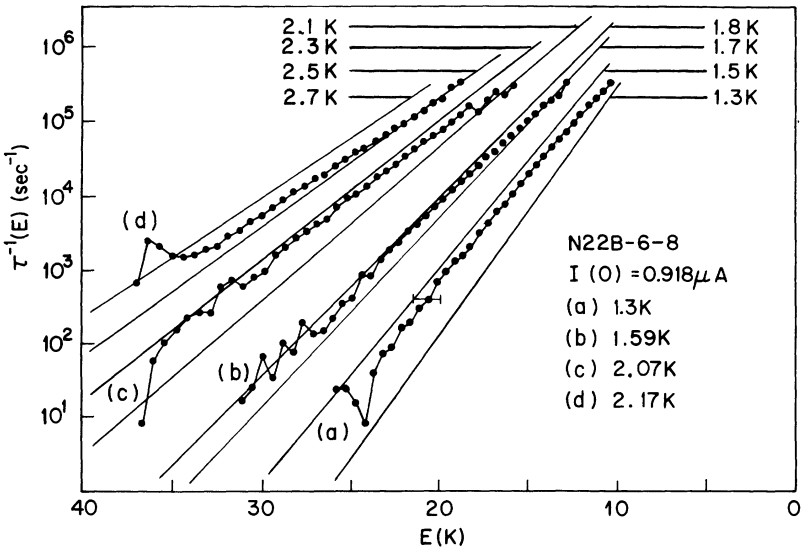

FIG. 6. Data points: $\log_{10}\tau^{-1}(E)$ vs E for junction of Fig. 4. Solid lines: theoretical dependence of $\log_{10}\tau^{-1}(E)$ on E for $\bar{\omega}_J/2\pi = 6.79\times10^8\,[I_c(1-x^2)^{1/2}]^{1/2}$ with I_c measured in μA. Note that generally the temperatures chosen for the theoretical plots exceed the bath temperature by ~0.1–0.2 K.

= 2.07 K the presumed critical current was I_c = 0.797 μA, giving a maximum energy barrier (at $I=0$) of 38.0 K. The observed I_{c0} ranged from 0.020 to 0.354 μA, or from $x=0.025$ to $x=0.444$, about two-fifths of the possible range, with $\tau^{-1}(I)$ varying from $\approx 5\times10^1$ to $\approx 5\times10^5$ at these two extremes. The energy barriers at the two extremes are 38 and 15.5 K, about three-fifths of the total range. Thus at one temperature the data cover a fairly broad range of possible parameters for this junction. The attempt frequency $\bar{\omega}_J/2\pi$ was $\approx 5.9\times10^8$ Hz for this range of x. Thermal-activation theory would predict that the inverse lifetime in this range would vary from ~5 to 3×10^5 Hz, which is roughly as observed. An effective noise temperature of as little as 5 K, on the other hand, would cause the inverse lifetime at $x=0$ to be of order 3×10^5 Hz with increasing values as x increases. For this low-current junction, then, the measured $\tau^{-1}(I)$ is a sensitive function of noise temperature, and comparison with theory is fairly stringent.

The solid lines in Fig. 6 show the predicted values [from (3) and (4)] of $\log_{10}\tau^{-1}(I)$ for various assumed noise temperatures. For curves (a)–(c), taken for T below the λ point, the data are in near-agreement with the activation expression if one adopts a noise temperature which exceeds the bath temperature by ~0.2 K. Four other similar sets of data, not shown, were taken in this temperature region and showed similar results. Four curves taken above the λ point, including curve (d) of Fig. 7, showed effective noise temperatures exceeding the bath temperature by ~0.5 K. This is a general feature of the junctions studied, and suggests that the junctions may be somewhat warmer than the bath temperature when not cooled by the superfluid film condensed from the exchange gas.

Although the experimental curves of $\tau^{-1}(E)$ are bounded by theoretical curves based on an effective temperature close to the bath temperature, an attempt to fit them with a best straight line would result in a slightly higher effective temperature and an attempt frequency about a factor of 2 smaller than $\bar{\omega}_J/2\pi$. As we shall describe subsequently, extrinsic noise in our experiments was generally somewhat nonthermal. Thus it is probably not valid to draw conclusions from such a fit.

It is interesting to see to what extent the data of Fig. 7 are in agreement with the predicted dependence of the energy barrier E on current bias I (Fig. 3). If we assume the noise temperature and the bath temperature are the same, we can derive from (3) and the experimental $\tau^{-1}(I)$ a value for $E(I)$. Figure 7 shows a plot of $E(I)/(I_c\Phi_0/\pi)$ versus I/I_c derived in this way for the data sets (a) and (c)

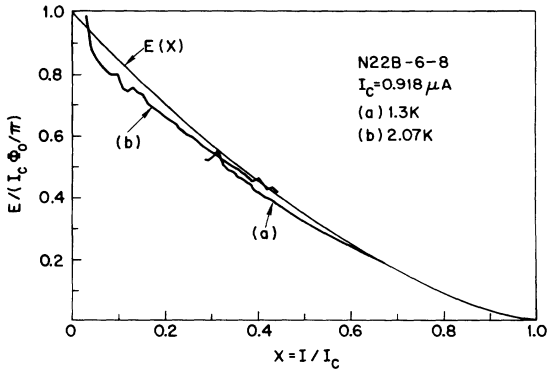

FIG. 7. Plot of $E/(I_c\Phi_0/\pi)$ vs x as derived from the data of Figs. 4 and 6 and the theory of Fig. 2.

of Fig. 4. The light line is the theoretical value of this quantity, as in Fig. 2. The agreement is fairly good.

It has been assumed in the preceding analysis that the junction voltage will increase to the steady-state value each time the junction escapes from the potential well. This ignores the possibility that noise-induced fluctuations in the "kinetic energy" ($\frac{1}{2}CV^2$) may cause the junction to be retrapped in a potential well and reenter the $V=0$ state. If x is of order $4(\pi\omega_J\gamma)^{-1}$, the minimum value at which $V\neq 0$ can occur in the noise-free picture, then this process is certainly important. Indeed it is probably the mechanism which causes the familiar discontinuous return from $V\neq 0$ to $V=0$ at small x in tunnel junctions.[6] For larger values of x, corresponding to $\frac{1}{2}CV^2 \gg kT$ in the steady state, we expect intuitively that noise-induced retrapping would be most likely to occur in the potential well immediately below that from which the escape occurs. In this regime the average value of $\frac{1}{2}CV^2$ increases by $I\Phi_0$ (~150 K for $I=1$ μA) for each 2π increase in φ. The time required for φ to increase by 2π after the escape is several small oscillation periods ($2\pi/\omega_J$), and the time scale of the energy fluctuations must be comparable to or larger than this. As a rough estimate, retrapping might have a significant chance of occurring if $I\Phi_0 \sim kT$, or $I\sim 10^{-8}$ A. This regime is approached in the small-I portion of Fig. 4, but the data do not show any obvious tendency for anomalously small numbers of counts in $P(I)$ in this regime.

Near-thermal-noise-limited critical currents have been observed on four other junctions having critical currents of 1.51, 5.86, 6.18, and 13.30 μA. For the higher critical currents, however, the deviation of I_{c0} from I_c is only of the order of 10%, so that systematic or random errors in measurement affect the comparison with theory. For the larger values of I_c, however, the values of $E(I)$, and hence $\tau(I)$, depend strongly on the quantity $\Delta I = I_c - I$ but only weakly on the individual values of I and I_c for fixed ΔI. Thus, for example, I_c at a particular temperature may be chosen as a single adjustable parameter and the value of $\tau(I)$ at other temperatures can then be computed and compared with experiment. Another approach[7] is to note that the temperature enters the problem as a scaling factor in the large-I_c case, so that approximately the linewidth of $P(I)$ should vary as $T^{2/3}$. This analysis is that used by Jackel *et al.*[13,14]

B. Extrinsic noise

A number of measurements of $P(I)$ for junctions mounted on less well-shielded sample holders showed the behavior in which extrinsic noise was a dominant factor. The level and characteristics of the noise in each case vary with the details of the electrical transmission characteristics of the sample holder, and therefore are not of intrinsic interest. Nevertheless, some general conclusions could be drawn.

Figure 8 shows two $P(I)$ and the corresponding $\log_{10}\tau^{-1}(I)$ taken at different temperatures for junction N20A-4-10. The effective noise level was well above thermal with $T_N \sim 3.0$–3.5 K. A near-exponential dependence on I occurs in portions of the data, but a well-defined kink is present in the central portion of the curve, indicating nonthermal noise. The inset of Fig. 8 plots the square of the current at the kink for these and several other runs at various temperatures versus I_c^2. The near-linear dependence indicates that the kink occurs when the attempt frequency $\bar{\omega}_J/2\pi$ is at the fixed value

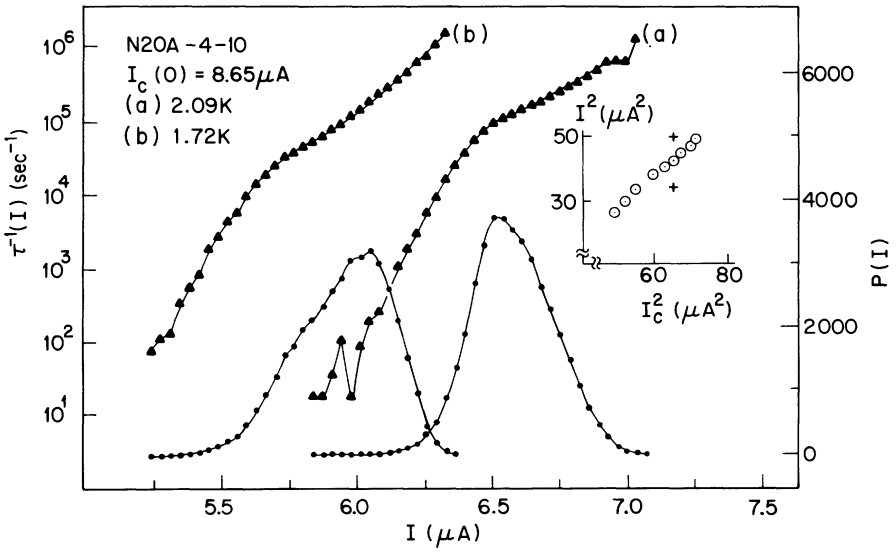

FIG. 8. $P(I)$ and $\log_{10}\tau^{-1}(I)$ vs I for junction N20A-4-10. Sweep frequency was 499 Hz and sweep amplitude was 9.85 μA. Inset: Circles, square of current I at which a kink in $\tau^{-1}(E)$ occurs plotted against square of the critical current I_c. Each point corresponds to a different temperature. Crosses, extreme values of I^2 at which I_{c0} occurred at one particular temperature.

1.82×10^9 Hz, which may be an electrical resonance of the 41-cm-long exchange-gas chamber. In this particular case, then, the extrinsic-noise spectrum is not flat but possesses at least one well-defined peak of estimated $Q\sim 50$ from the kink width. Most probably, the spectrum possesses a series of such sharp peaks at the various resonances of the sample holder. Nonetheless, if the range of measurable $P(I)$ does not happen to overlap with one of these, the values of $\tau^{-1}(I)$ often show near-exponential dependence on energy, from which one could mistakenly derive an attempt frequency and effective temperature.

V. SUMMARY

We have described here a series of experiments which measure the probability distribution of observed critical currents in Sn-Sn Josephson tunnel junctions. These data were used to determine the lifetime τ of the zero-voltage state of the tunnel junction as a function of current bias I. Values of τ from $>10^{-1}$ to $\approx 10^{-7}$ sec were observed for single junctions, showing an approximately exponential decrease with I. A determination of the constant of proportionality between the resistance of the I-V curve in the superconducting state and the true critical current enabled us to determine τ as a function of the energy barrier against activation. For adequately shielded samples the lifetimes were in near agreement with thermal-activation theory, with attempt frequencies in the GHz range and energy barriers of from 40 to 10 K in the range of obserable τ. Extrinsic noise of nonthermal character was observed in less well-shielded samples.

For most of the junctions described here the plasma frequency ω_J was small enough that a classical picture of the activation is undoubtedly proper. One of the smaller-area junctions investigated, for which near-thermal behavior was observed, had $\hbar\omega_p/k\approx 0.3$ K, which may be on the border of the regime for which quantization of the classical Josephson electrodynamics is observable. No unusual behavior was observed in this junction, however. We are presently continuing this work with a view to investigating regimes of larger $\hbar\omega_J$.

ACKNOWLEDGMENTS

We wish to thank R. A. Logan and V. Narayanamurti for the use of equipment and W. W. Webb and J. E. Lukens for furnishing us with preprints of Refs. 13 and 14.

[1]Y. H. Ivanchenko and L. A. Zil'berman, Zh. Eksp. Teor. Fiz. 55, 2395 (1968) [Sov. Phys.-JETP 28, 1272 (1969)].
[2]V. Ambegaokar and B. I. Halperin, Phys. Rev. Lett. 22, 1364 (1969).
[3]A. M. Goldman, J. Low Temp. Phys. 3, 55 (1970).
[4]P. A. Lee, J. Appl. Phys. 42, 325 (1971).
[5]M. J. Stephen, Phys. Rev. 182, 531 (1969); Phys. Rev. 186, 393 (1969).
[6]J. Kurkijärvi and V. Ambegaokar, Phys. Lett. 31A, 314 (1970).
[7]J. Kurkijärvi, Phys. Rev. B 6, 832 (1972).
[8]V. E. Kose and D. B. Sullivan, J. Appl. Phys. 41, 169 (1970).
[9]H. Ohta, J. Appl. Phys. 43, 5161 (1972).
[10]J. T. Anderson and A. M. Goldman, Phys. Rev. Lett. 23, 128 (1969).
[11]M. Simmons and W. H. Parker, Phys. Rev. Lett. 24, 876 (1970).
[12]W. A. Henkels and W. W. Webb, Phys. Rev. Lett. 26, 1164 (1971).
[13]L. D. Jackel, J. Kurkijärvi, J. E. Lukens, and W. W. Webb, in *Proceedings of the Thirteenth Low Temperature Conference, Place*, 1972, edited by R. H. Kropschot and K. D. Timmerhaus (University of Colorado Press, Boulder, Colo., 1973).
[14]L. D. Jackel, W. W. Webb, J. E. Lukens, and S. S. Pei, Phys. Rev. B 9, 115 (1974).
[15]A. J. Dahm, A. Denenstein, D. N. Langenberg, W. H. Parker, D. Rogovin, and D. J. Scalapino, Phys. Rev. Lett. 22, 1416 (1969).
[16]H. Kanter and F. L. Vernon, Jr., Appl. Phys. Lett. 16, 115 (1970); Phys. Rev. Lett. 25, 588 (1970).
[17]G. Vernet and R. Adde, Appl. Phys. Lett. 19, 195 (1971).
[18]H. Kanter and F. L. Vernon, Jr., Phys. Rev. B 6, 4694 (1970).
[19]B. D. Josephson, Phys. Lett. 14, 251 (1962).
[20]P. W. Anderson and J. M. Rowell, Phys. Rev. Lett. 11, 80 (1963).
[21]W. C. Stewart, Appl. Phys. Lett. 12, 277 (1968).
[22]D. E. McCumber, J. Appl. Phys. 39, 3133 (1968).
[23]S. A. Buckner, J. T. Chen, and D. N. Langenberg, Phys. Rev. Lett. 25, 738 (1970); see also T. A. Fulton, Phys. Rev. B 7, 1189 (1973).
[24]S. Chandrasekhar, Rev. Mod. Phys. 15, 1 (1943).
[25]H. Kramers, Physica 7, 284 (1940).
[26]P. W. Anderson, in *Lectures on the Many-Body Problem*, edited by E. Caianello (Academic, New York, 1964), p. 115.
[27]For example, K. Schwidtal and R. D. Finnegan, Phys. Rev. B 2, 198 (1970); I. K. Yanson, Zh. Eksp. Teor. Fiz. 58, 1497 (1970) [Sov. Phys.-JETP 31, 800 (1970)].
[28]I. Giaever, Phys. Rev. Lett. 5, 147 (1960); Phys. Rev. Lett. 5, 464 (1960).
[29]This applies primarily to the TEM modes.
[30]M. D. Fiske, Rev. Mod. Phys. 36, 221 (1964).
[31]T. A. Fulton and D. E. McCumber, Phys. Rev. 175, 585 (1968).
[32]V. Ambegaokar and A. Baratoff, Phys. Rev. Lett. 10, 486 (1965); Phys. Rev. Lett. 11, 104(E) (1965).
[33]S. Paley, J. Wilson, and R. I. Gayley, Phys. Lett. 41A, 311 (1972).
[34]B. Mühlschlegel, Z. Phys. 155, 313 (1959).
[35]J. C. Swihart, J. Appl. Phys. 32, 461 (1961).

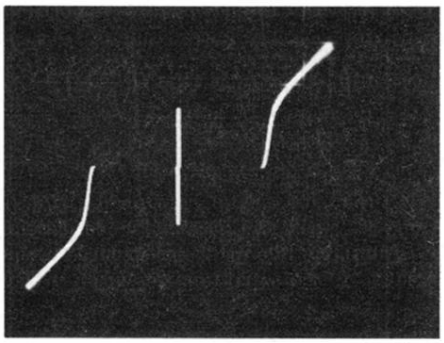

(a)

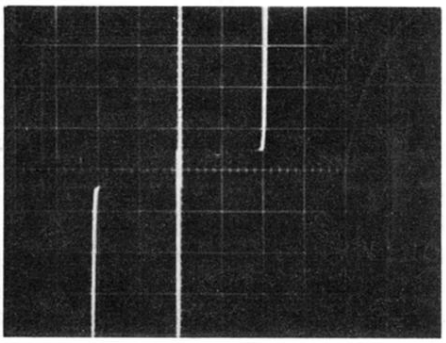

(b)

FIG. 3. Current-voltage characteristics of junction 31A-5-9. (a) 500 μA/vertical division and 0.5 mV/horizontal division. (b) 10 μA/vertical division and 0.5 mV/horizontal division. Temperature = 1.4 K.